PIK-20D Glider Fatigue Review

Erkki Soinne
erkki.soinne@traficom.fi
Finnish Transport and Communications Agency, Helsinki, Finland

Abstract

A fatigue inspection program has been established for the PIK-20D glider. This paper explains the reasoning for the inspection interval and the inspection objects. As a basis for this the stress calculations, fatigue and material tests and drawings of PIK-20D were reviewed. A noticeable effort was made to collect all relevant material data derived in the 1970s. The fatigue calculations performed were reviewed and the results were transformed to be consistent with the Kossira-Reinke spectrum, which has become a standard in Europe. The effect of aerobatic flight on fatigue was investigated. The review covers the entire glider with emphasis on the wing composite spar and web and the primary metal brackets. The review shows a long fatigue life and that there are no known fatigue problems on PIK-20D.

Introduction

Fatigue of composite gliders has been studied in several countries such as Australia and Germany. In the 1960s Franzmeyer derived an analytic fatigue spectrum for gliders and a fatigue test was performed on a Cirrus glider [1]. Kossira and Reinke performed flight measurements in the 1980s to establish an envelope spectrum covering all types of glider flights [2]. To enable the extension of fatigue life of gliders, Patching and Wood performed in the 1990s flight load measurements and a fatigue test on a Janus wing [3].

Composite glider fatigue has been studied by many investigators. Of the numerous references here are mentioned those by Kensche on life time prediction and certification [4–7]. Waibel has written a valuable summary on the subject [8].

The first fatigue test in Finland was performed on a PIK-20 glass fiber wing in 1974. Material fatigue tests were made on PIK-20B wing spar cap carbon fiber laminate and a test followed on a PIK-20D carbon fiber wing in 1977, see Nyström and Mai [9]. Fatigue tests or calculations were not required in the OSTIV airworthiness requirements [10], which were used in the certification of PIK-20D in the utility category. Later on, PIK-20D was approved, also by EASA, for the aerobatic category.

Fatigue is a common question for all aging aircraft and it is wise to plan in advance for possible actions. The European safety agency EASA has requested the Finnish Transport Safety Agency Trafi to make a fatigue inspection program for the PIK-20D glider. As a basis for the inspection objects and inspection interval the stress calculations, fatigue and material tests were reviewed and new fatigue calculations were made for the primary metal brackets.

Presented at XXXIII OSTIV Congress, Benalla, Australia, 8-13 January 2017.

This paper first describes the PIK-20D structure. Then, a critical review is made on the fatigue calculations based on the methodology used at Saab on commercial and military aircraft. The method is applied on the composite wing spar cap and web fatigue calculations. The results are transformed to be consistent with the Kossira-Reinke spectrum. Also the effect of aerobatic flight is investigated. The effect of the stress levels in the performed static and fatigue tests is assessed. The fatigue of the primary metal brackets is calculated using the Saab method. Finally the factors influencing the inspection program are described.

PIK-20D Structure

The PIK-20D glider, shown in Fig. 1, is made of glass fiber epoxy composite with the wing spar caps in carbon fiber, as shown in Fig. 2. The resin used is the Rütapox L02/SL sys-

Fig. 1: PIK-20D in flight.

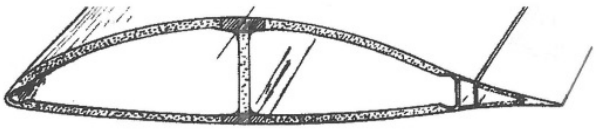

Fig. 2: PIK-20D wing section structure.

tem, which was cured at a temperature of 70° C, thus permitting the use of colored external surface paint. The wings and tail surfaces have a sandwich structure with PVC foam core. The paint is a two component epoxy paint (used on icebreaker ships) giving a more durable protection than gelcoat.

The glider wing rigging is shown in Fig. 3. The spars are assembled together so that the four beveled shear pins 4, 5, 6 and 7 on the wing root ribs move into the corresponding bushes in the fuselage and the spar end pins into the bushes in the other wing root ribs. The rigging is secured with the main wing pin 3 inserted through the wing spars at the fuselage center line.

The horizontal tail rigging, shown in Fig. 4, begins by installing the tail bushes 1 and 2 on the fin two aft bracket pins 3 and 4. Then the movable pin 5 on the fin forward bracket is opened, the horizontal tail forward part with the bracket rod end is turned down against the fin upper end and the movable pin is inserted through the rod end. The flap, airbrake and elevator controls are connected manually.

Calculation of fatigue life

In the calculation method, used at Saab on metal structures fatigue of civil and military aircraft, the cumulative damage sum D is determined according to the classical Miner-Palmgren rule

$$D = \sum_{i=1}^{k} \frac{n_i}{Ni} \tag{1}$$

where n_i is the number of load cycles and N_i the number of allowable load cycles at a certain stress level. The method contains five steps (see ref. [11] Holm chapter 11).

- treatment of the loading spectrum
- normal correction of the coupon* fatigue tests
- application adjustment
- scatter factors for life and stress
- choice of the cumulative damage sum D

In the first step the loading spectrum, based on the average use of the aircraft, is modified so as to cover the limit fatigue loads that the aircraft will experience. Often at Saab the loads have been increased by a factor of 1,5 in load cycles (at low number of cycles) and by a factor of 1,15 in stress (at high number of cycles).

In the second step of normal correction the coupon fatigue test results are corrected to take into account the scatter between different material batches. In the Saab methodology the average curve results are reduced to a level so as to cover all values above the lower quartile of the average values.

In the third step of application adjustment the Saab method takes into account differences between the material coupon test data and the analyzed application case. In metal structures the following factors are of interest: stress concentration, size of the test coupon (a small coupon has higher fatigue stress values in metallic materials) and surface effects (such as surface roughness, surface treatment, heat treatment, fretting and corrosion). In the application adjustment procedure for metal structures the allowable stress amplitude σ_a is expressed as

$$(\sigma_a)_2 = (\sigma_a)_1 \frac{\alpha_1}{\alpha_2} \Psi \tag{2}$$

*Editorial note: In the field of materials science tensile test specimens are often called coupons.

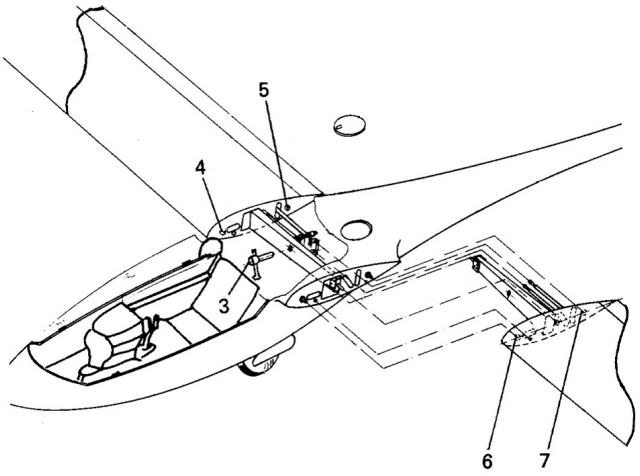

Fig. 3: PIK-20D wing/fuselage joint.

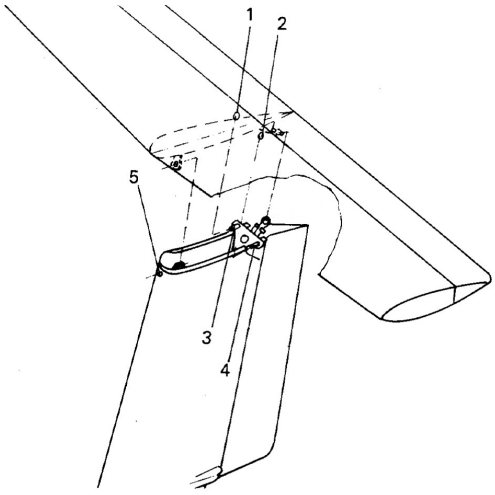

Fig. 4: PIK-20D horizontal/vertical tail joint.

where index 1 refers to the material test values and 2 to the application adjusted values. α is the stress concentration factor and Ψ is a factor taking into account surface effects such as machining, surface treatment, surface hardening, fretting and corrosion

$$\Psi = \delta \cdot \kappa_m \cdot \kappa_s \tag{3}$$

where κ_m is a factor due to surface roughness (due to machining, lathing, polishing etc) and κ_s due to surface treatment (such as an anodic oxidization or an alodine process). δ is the volume factor

$$\delta = \left(\frac{V_1}{V_2}\right)^{1/m} \tag{4}$$

where V_1 is the stressed volume in the material test coupon and V_2 in the application and m in the exponent is a material parameter. For steel $m = 30$. The stressed volume may be expressed as

$$V = \rho^2 \cdot \lambda \cdot c \tag{5}$$

where ρ is the radius of the notch**, λ the material thickness at the notch and c is a constant. The surface effect factor is assumed to have full effect at $N = 10^6$ cycles and the value 1,0 at $N = 10^1$ with linear interpolation on a log scale in between and constant values beyond.

In the fourth step scatter factors are applied on a metal structure fatigue curve to account for the uncertainty of the fatigue calculations and the scatter in the fatigue tests within the tested material batch or full scale test. A factor is applied on the application adjusted fatigue curve of step three either in number of cycles at low values of cycles (a life factor) or in stress level at high values of cycles. Typical values of $f_N = 3$ in life and $f_S = 1{,}3$ in stress level are quoted. A factor of life of 3 implies a risk to fracture of about 0,001 and a factor of 4 a risk to fracture of about 0,00001, Jarfall [12] (page 97).

In the fifth step the limit value for the cumulative damage sum D is chosen, that corresponds to the fracture of the structure. Jarfall [12] (page 104) gives examples of values on D corresponding to fracture in metal structures in a number of examples. The example values range from 0,12 to 3,8. At Saab the following values have been used in fatigue calculations of metal structures:

$D = 0{,}5$ in structures loaded with stress ratio $R = -1$

$D = 0{,}7$ in structures with other stress ratios

$D = 1{,}0$ for lugs with other stress ratios

It is also stated in the Saab fatigue methodology that "superposition of all individual effects in fatigue must be made with careful consideration so that the overall effect becomes realistic and well balanced". Experience and engineering judgment are invaluable in fatigue analysis.

The following factors have an influence on composite structures fatigue:

- load spectrum
- aerobatic flight
- resin system and fiber type
- material survivability and confidence limits
- application adjustment
- scatter factors for life and cumulative damage sum

and will be taken into account in the analysis as follows:

Load spectrum

The following loading spectra have been used in the fatigue tests or analysis of PIK-20 gliders:

- Keturi
- Nyström
- Nyström with 44% increased strain levels
- Royal Melbourne Institute of Technology
- Franzmeyer
- Kossira-Reinke

A comparison of the spectra is shown in Fig. 5.

The gust loads in the Nyström spectrum were derived using power spectral density analysis. In the PIK-20D fatigue test the loads were scaled up 44% to deliberately apply a very conservative spectrum. All results have now been transformed to the Kossira-Reinke spectrum to ease comparison with other gliders.

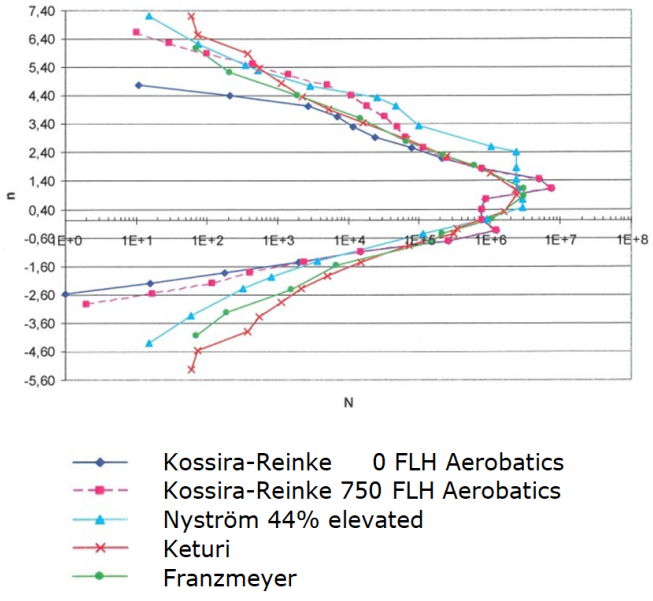

Fig. 5: 6000 Flight hour (FLH) loading spectra for PIK-20D, Lukkarinen [13] (page 96).

**Editorial note: A notch is a geometric discontinuity that leads to stress concentration and, thus, reduces tensile strength of any load bearing structural element.

The Kossira-Reinke spectrum is based on flight load measurements. It constitutes a conservative envelope spectrum as it is intended to cover all types of glider operations in a single spectrum (flight training with two-seaters, cross country flying, mountain flying, wave flying etc). The spectrum is considered to be "very much to the conservative side despite an omission of low amplitude cycles", Waibel [8].

The spectrum contains the treatment of limit fatigue loads as the measured flight loads have been extrapolated to contain the maximum loads during the aircraft life time. However, the extrapolation has been performed, not to the 6000 FLH spectrum life time target, but conservatively to 6000 FLH times a life factor 3, generally used in glider fatigue tests in Germany, Kossira and Reinke [2] (page 46). Besides a normal life factor conservatism has also been used in the extrapolation resulting in a double effect. However, the effect of the extrapolation is not large. The spectrum is treated principally in the same way as in the Saab method and constitutes the limit fatigue loads that a glider will experience.

Aerobatic flight

In the measurement of the flight loads for the Kossira-Reinke spectrum a maximum load factor of $n = 6{,}62$ was reached in a badly performed aerobatic maneuver. Due to a selected high design value for the maximum speed in gusty weather V_B the PIK-20D V,n-diagram covers this value. Consequently the glider has an appropriate margin for pilot mistakes in aerobatic maneuvers.

The Kossira-Reinke spectrum has a variant where 12,5% of aerobatic flight has been added (750 FLH aerobatics to a 6000 FLH spectrum) and thus the effect of aerobatics on fatigue can be studied. As is seen in Fig. 5 aerobatics has a noticeable effect on the spectrum at high load factors. Just adding aerobatic flight to the spectrum, instead of replacing some other type of flight, increases the conservatism of the spectrum.

Resin system and fiber type

The fatigue properties of a composite material depend on the fiber type, resin system and the production process.

A major factor influencing the fatigue properties of the laminate is the resin shear modulus and the curing temperature. The resin shear modulus for different epoxy resins is shown in Fig. 6. Increasing the curing temperature increases the stability of the resin (the shear modulus G) at high temperatures. Epikote 162 resin shows the least stability with increasing temperature. The temperature that white gliders reach in sunlight is 54° C and at this temperature the shear modulus is only about half of the value at 15° C. This means that the postcuring continues which is shown for example on the wing surfaces, where the patterns of the sandwich foam bondings appear in many older gliders. If the resin is not fully stabilized during the curing the fatigue properties are less good.

PIK-20 series gliders were made of the Rütapox L02/SL system, cured at 70° C. After 40 years there is still no sign of the foam pattern on the wing skins. At elevated temperatures there is only a minor reduction in the resin shear modulus.

In the material acceptance tests of the Luftfahrt Bundesamt, performed at the DFVLR research institute in 1974 and 1975, the Rütapox L02/SL system showed over a factor 100 more cycles to failure than the GE162/C260 resin system commonly used in gliders, Lumppio [15] (page 131).

Also the production method has an influence on the produced composite material. The spar caps on PIK-20D were fabricated from Courtaulds Grafil A-S carbon fiber and Rütapox L02/SL resin system. A bundle of tows was pulled through a resin basin and a nozzle and placed into the spar cap tool, where pressure was applied on the material during curing. The method guaranteed a 60% fiber volume and a void free even quality.

Fatigue tests on the PIK-20D carbon fiber spar cap material were performed at Helsinki University of Technology (now Aalto University) in several phases using a fatigue bending test and a stress ratio R=-1. First the test coupons were sawed from fabricated spar caps thus cutting through the filaments at the coupon surfaces. On a 2 mm thick coupon this brought a reduction in the fatigue strength. To avoid cutting through the fibers, the test coupons were later on cured under pressure in the same way as on the PIK-20D wing spar to directly produce the test

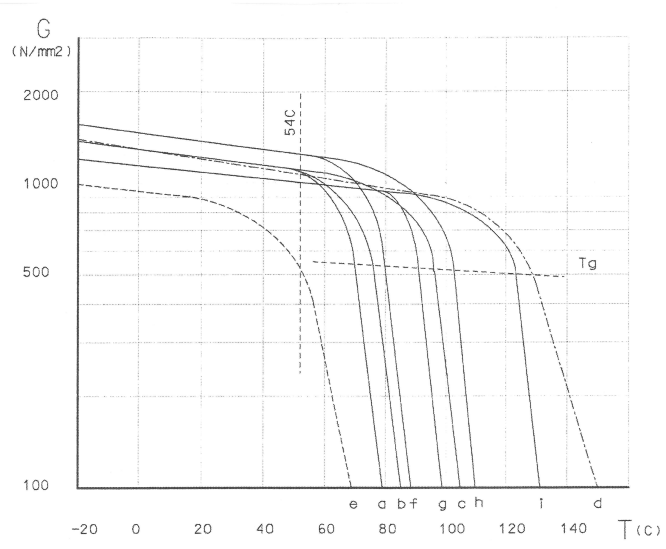

kuva C8 Eri epoksihartsien liukumoduli G lämpötilan funktiona

a) L285 + Hä285 24h 20°C + 15h 50°C
b) L285 + Hä287 24h 20°C + 15h 50°C
c) L285 + Hä287 24h 20°C + 15h 80°C
d) Ly5052 + Hy5052 24h 20°C + 15h 80°C
e) Epikote 162 + Epikure 113 24h 20°C + 15h 60°C
f) Rütapox L02 + H91 24h 20°C + 15h 50°C
g) Rütapox L02 +SL50 24h 20°C + 15h 70°C
h) Rütapox L02 + H91 24h 20°C + 15h 70°C
i) Rütapox L02 +SL 24h 20°C + 15h 110°C

Fig. 6: Shear modulus G of epoxy resins as function of temperature and postcuring time, Korhonen [14] (page64).

coupon thickness. Both sets of results are presented in Fig. 7 together with the S-N curve of Sigri NF12 carbon fiber and the Shell GE163/C260 resin system.

The coupons cured under pressure directly to the final thickness (filled circular symbols) did not break (runout) at 10^7 cycles at any of the three test strains. At 10^7 cycles the PIK-20D spar material sustains at least a strain of 0,667% whereas the corresponding value for the Sigri NF12 and Shell GE163/C260 laminate is 0,400%.

Material survivability and confidence limits

In the second step of the Saab method a normal correction of the coupon fatigue tests is performed by reducing the average values to lower quartile values. It is not known if the PIK-20D test coupons contained specimen from different material batches. However, the fatigue curve encloses all coupon tests and all of them were unbroken runouts. Thus, it is concluded that the Saab method principle of using lower quartile values is fulfilled.

Application adjustment

In composite structures relevant factors in application adjustment are stress concentration, size of the test coupon, composite material production process and stress ratio.

The spar caps of PIK-20D are slightly S shaped just outside the root rib as the wing spar structural height is reduced inboard of the rib. The effect of this has been studied with a finite element method model, shown in Fig. 8. A close up view of the upper wing spar cap strains is shown in Fig. 9. The computations are within 10% of the strain gage measurements and show a peak in the distribution just outboard of the root rib. The computed strain peak of $\varepsilon = 0,5393\%$ at maximum limit load is taken into account in the fatigue life computations. The maximum limit load strain occurs at the maximum take-off weight of 450kg and load factor $n = 6,62$.

A stress concentration arises usually in a notch and the test coupon has to simulate the application. In the case of PIK-20D wing spar there is no notch but a mild stress concentration due to the abrupt stiffness and a geometry change in the structure in the vicinity of the root rib. As the maximum strain is used

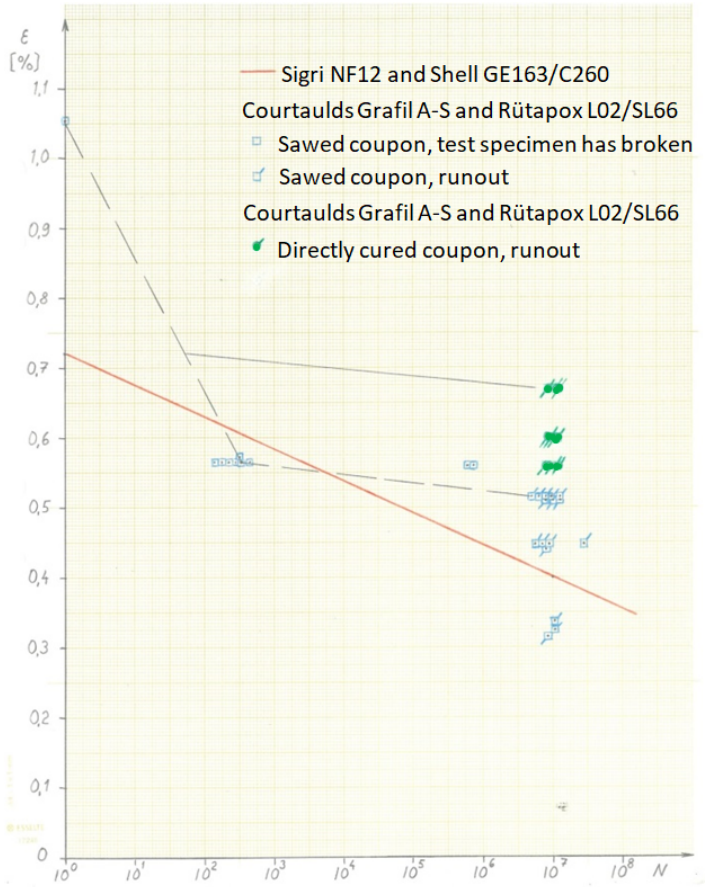

Fig. 7: Wing spar composite carbon fiber material fatigue strains as function of number of cycles, Soinne [3].

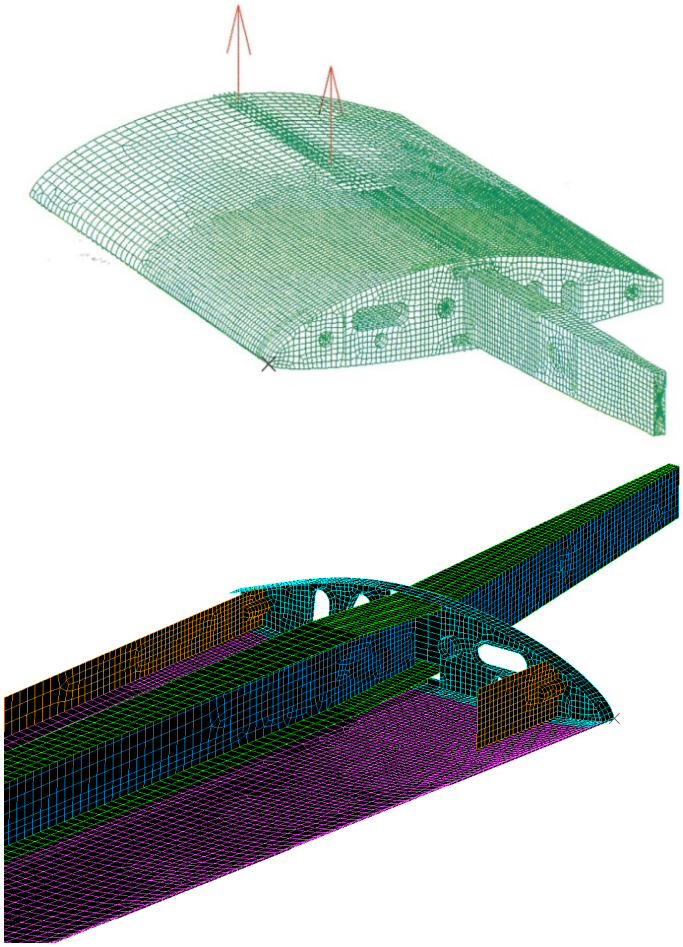

Fig. 8: PIK-20D wing root area strucure FEM model, Lukkarinen [13] (page 33 and 66).

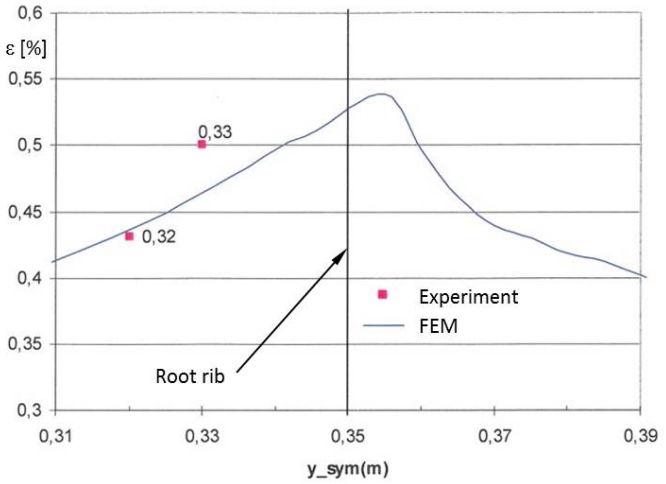

Fig. 9: PIK-20D upper spar cap strains computed at limit load n=6,62 and maximum weight m=450 kg with a FEM model (FEM) and measured in the static test (Experiment). The numbers indicate the strain gage location from the symmetry axis, Lukkarinen [13] (page 70).

in the fatigue calculations the effect of stress concentration is appropriately handled in the calculations.

The size of the test coupon has an effect on the fatigue properties. In composite coupons the effect is reversed to that of metal coupons. It is known, that composite structures coupon tests yield conservative results compared with component tests such as a wing, Waibel [8] (page 59). Consequently the PIK-20 fatigue calculations are conservative in this respect. Performing the tests with coupons, produced in the same way as the wing spar cap, takes properly into account the composite material production process.

Fatigue tests on the PIK-20D carbon fiber spar cap material were performed at stress ratio $R = -1$. In reality the stress ratio varies in a range of $-0{,}55... - 0{,}8$. Consequently using a stress ratio of $R = -1$ is conservative.

The application adjustment is made in line with the Saab method.

Scatter factors and cumulative damage sum

The limit value for the cumulative fatigue sum D shall be chosen so that it corresponds to the fracture of the structure. The Saab method follows this principle. There is a fairly large variation of the limit value D, which brings the calculations to match the test results. Kensche [6] quotes on page 47 that the value of D can vary from 0,1 to 10 for metals as well as for composites.

The FAA recommends that with analysis alone, without a structural fatigue test, a scatter factor of 8 in life is to be used together with a cumulative damage sum of $D = 1{,}0$ on metal structures, [16]. Even if the cumulative fatigue sum that fits best the failure of the structure may be somewhat lower, the FAA in a practical way puts all margins into a single factor.

Here the following approach is chosen. A cumulative fatigue sum value D, matching the structural failure, is used together with a life factor appropriate for calculation. Lacking better data the value $D = 0{,}1$ is used together with a life factor of 8. This approach is more conservative than the FAA and the Saab method.

Wing spar cap fatigue

The fatigue calculation in [17] using the Miner-Palmgren expression (1) gave for the spar cap of PIK-20D a fatigue life of $4{,}829 \cdot 10^{20}$ FLH. This result is based on

1. the Kossira-Reinke load spectrum with 12,5% aerobatic flight added,
2. the reduced S-N curve in Fig. 7 of Courtaulds Grafil A-S carbon fiber and Rütapox L02/SL66 resin system with the FEM method calculated peak stress,
3. the stress ratio of $R = -1$,
4. a life factor of 8 and
5. a cumulative fatigue sum of $D = 0,1$.

Only the highest load level at $n = 6,62$ contributes to fatigue. The result is still conservative due to the conservative choice of the limit value D and the conservative approximation in the stress ratio R. Also the aerobatic flight spectrum was handled conservatively as it was based on the maximum take-off weight of 450 kg, whereas aerobatics is flown without water ballast at a maximum weight of 360 kg. There is no indication of a fatigue problem in the wing spar.

Wing fatigue test

The development fatigue test on the PIK-20D wing, performed after the type certification approval, was made using the Nyström spectrum with 44% elevated strain levels, a 4000 FLH spectrum length and applying a scatter factor of 4 on life. Nystrms sequence fulfills the FAA guidance in [16] on load levels, sequence block size and order.

To create a more even strain distribution in the wing spar it was decided to locally reinforce the upper spar cap and the web forward side in the vicinity of the wing root. The maximum compression spar cap strain in the fatigue test wing then was reduced by 20,79%. As the maximum load level in the elevated Nyström sequence is $n = 6{,}24$ yielding a strain of $\varepsilon = 0{,}40266\%$ on the reinforced wing, the fatigue test in total was slightly less severe than the Kossira-Reinke spectrum with 12,5% aerobatics added. The intention of the Nystrm sequence was not to cover aerobatics as the PIK-20D was not initially approved for aerobatic flight.

Before reinforcing the wing root area, there were about 30 static loadings performed for calibration, strain measurement and deflection purposes. For the unreinforced wing a load case with a load factor $n = 6{,}62 + 20\% = 7{,}944$ was applied 9 times. The cumulative damage sum for the static cases can be calculated using the Miner-Palmgren rule (1). Considering the static

tests as the critical part of the Kossira-Reinke spectrum with 12,5% aerobatics added they cover a life of $2{,}893 \cdot 10^{14}$ FLH and were more severe than the fatigue test itself.

Increasing the load level in aircraft fatigue tests is an acknowledged way to reduce the time needed for the testing. Low loads are enhanced to a higher level thus permitting a reduction of the number of corresponding cycles. High loads cannot be enhanced to even higher levels as they would impair the results when metal components are exposed to yielding (plasticity). Sequences with high loads are, on the contrary, increased in number to increase the statistical confidence of the test. Due to the low number of the high loads the effect on the total time for testing is however negligible.

Tomblin and Seneviratne present in [18] a survey on the effects of the load enhancement factor and the life factor. Figure 10 shows the load enhancement factor as function of the test duration for a constant statistical confidence, based on three databases on composites fatigue data variability as well as on some material combinations.

To get a feel for the effect of increasing the loads by 20% use the average gradient of the data base curves to find out how large a change corresponds to in testing time (only the slope of the curve is relevant here). Use the gradient of the Navy data base, having the largest scatter in fatigue, as wet layup tends to have a higher scatter than prepreg production. A load enhancement factor 1,2 corresponds about to a factor 14 in testing time based on equal statistical confidence. This would mean that the performed static tests at the 20% elevated strain level with 9 high loads are equivalent to $(9/10) \cdot 6000 \cdot 14 = 75600$ FLH on the wing spar cap with a life factor of 1 in excess of the elevated Nyström spectrum.

The different estimates on PIK-20D fatigue life all give fairly high values. An explanation for the long fatigue life is that

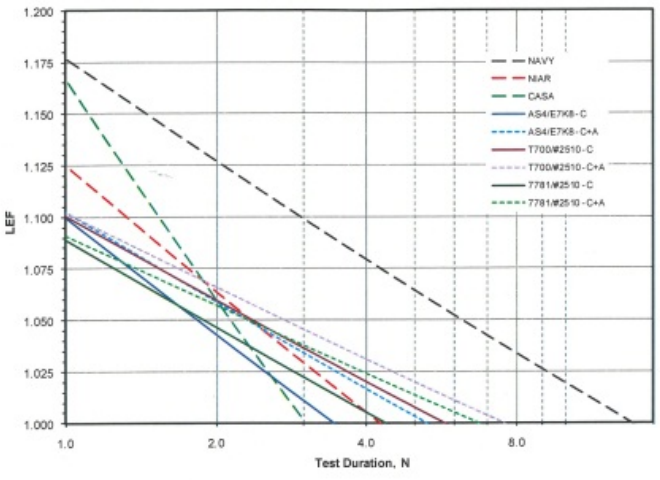

Fig. 10: Influence of test duration on B-basis Load Enhancement Factors (LEF) for different materials data bases, Tomblin and Seneviratne [18] (page80).

the chosen dimensioning strain level on the PIK-20D is fairly low. In the carbon fiber spar caps the intended maximum strain at limit load was 0,5% in fiber direction. The actual strain is 0,5393% at limit load in the strain peak in the spar cap just outboard of the root rib. This is over 10% lower than the value 0,61%, quoted in Kensche [5] (page 53) and Waibel [8] (page 58) as a common design level (limit strain) of a sailplane wing spar. The fatigue tests of the PIK-20D spar cap material showed that the material can sustain at least a strain of 0,677% for 10 million cycles.

Wing web fatigue

Kensche [5] has studied the fatigue of shear webs and his results indicate, that a wing spar web might be more critical than a spar cap.

In the wing spar web the stress state at the neutral axis is pure shear loading. The pure shear stress τ is equivalent to a state of acting stresses in the fiber directions

$$\sigma_1 = \tau$$
$$\sigma_2 = -\tau$$

in the $+45^\circ$ and -45° directions. The strain in fiber direction in this biaxial stress state can be derived as

$$\varepsilon = \frac{\sigma_1}{E_1} - \nu_{12}\frac{\sigma_2}{E_2} \tag{6}$$

where the first term is the strain due to the stress σ_1 in the principal 45° direction and the second term is the contraction due to the stress σ_2 in the perpendicular -45° direction. E_1 and E_2 are the moduli of elasticity in the fiber directions and ν_{12} is the Poisson number indicating contraction in direction 1 due to a stress acting in the perpendicular direction 2. The stress state is such that in the principal fiber direction the strain is ε and in the perpendicular direction the strain is $-\varepsilon$.

Strain measurements on the PIK-20D fatigue test wing indicated a higher strain on the forward side of the spar web than on the aft side. This probably was due to a locally asymmetric reaction to the wing spar end pin load in the root rib. The highest strain in 45° fiber direction at limit load $n = 6{,}62$ at the spar neutral axis was $\varepsilon = 0{,}492\%$. This is the limit load strain that can be compared with the normal corrected S-N curve of Fig. 11.

The S-N curve is valid for a biaxial stress state, in which the principal strain is ε and in the perpendicular direction the strain is $-\nu\varepsilon$. Thus the stress states in the wing spar web and the test coupon are not exactly equal, but in the principal direction the strains are the same. Another difference between the wing spar web and the fatigue test is in the weaves. The wing spar web was made of Interglas 92125 weave with 50% of the fibers in the principal direction and 50% in the perpendicular direction. The fatigue test coupon was made of Interglas 92145 with 90% of the fibers in the principal direction and 10% in the perpendicular direction. In a $0^\circ/90^\circ$ layup the amount of fibers is however the same in both directions.

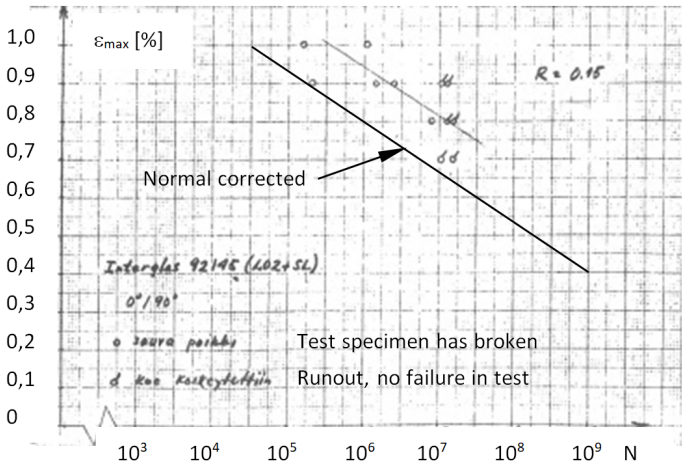

Fig. 11: S-N curve of $0°/90°$ symmetric glass fiber laminate with Interglas 92145 cloth and Rütapox L02/SL resin system. The test was performed using a tension test coupon. The stress ratio has a value $R = 0{,}15$ and ε_{max} is the maximum strain in the cycle in the coupon $0°$ direction, Soinne [17] (page 27).

The secondary effect of web vertical compression due to wing bending was ignored. The web bonding is lightly loaded and was not studied in this work.

The stress ratio of $R = 0{,}15$ implies that the maximum load is 6,67 times higher than the minimum load. This simulates quite well the wing maximum load cycles due to gust loads and maneuvering loads. A shortcoming in the test is that it only covers the tension loads in the principal direction.

The fatigue calculation in [17] (page 29) gave for the wing spar web of the PIK-20D a fatigue life of 938156 FLH. This result is based on

1. the Kossira-Reinke load spectrum with 12,5% aerobatic flight added,
2. the reduced S-N curve in Fig. 11 of Interglas glass fiber weave and Rütapox L02/SL resin system,
3. the stress ratio of $R = 0{,}15$,
4. a life factor of 8 and
5. a cumulative fatigue sum of $D = 0{,}1$.

The largest contributions to the fatigue emerge from low load levels at $n = 1{,}1 \ldots 1{,}47$ where aerobatic flight is not a factor. The estimate is very conservative as the S-N curve used is more severe than a lower quartile curve and the log-linear extrapolation to very high number of cycles, where the log-linear line unphysically crosses the zero strain level. There is no indication of a fatigue problem in the wing spar web.

Metal brackets fatigue

Fatigue calculations have not been required in the airworthiness requirements for glider metal parts. Nevertheless, the primary brackets were checked with the method utilized at Saab for commercial and military aircraft.

The brackets studied are the wing spar end main fitting, the wing bevel pins, the tailplane forward fitting and the fin forward and aft fittings. As examples of the calculations, the analysis of the wing spar end main fitting and the tailplane forward fitting brackets are presented. There was no cumulative fatigue sum on the wing bevel pins and the fin forward and aft fittings and thus no risk for fatigue.

Wing spar end main fitting

The wing spar end main fitting is an AISI 4130 alloy steel construction, quenched and tempered to a Tensile Ultimate Strength of $TUS = 100\,\text{kp/mm}^2$ (142,2 ksi or 980,7 Mpa).There is a lathed pin welded to the fitting plate which is bolted to the composite spar end. The critical section in bending is inside of the pin 3,5 mm flange at the junction of the 22 mm cylindrical part and the beginning of the 1 mm radius as shown in Fig. 12.

The material S-N curves are derived for a stress concentration factor $\alpha = 2{,}0$, a value closest to the actual value $\alpha = 1{,}717$. The material data utilized were taken from MIL-HDBK-5J, [19], for 4130 Sht Norm, $KT = 2{,}0$, $TUS = 120\,\text{ksi}$ and 4130 Sht Hard, $KT = 2{,}0$, $TUS = 180\,\text{ksi}$. The S-N curves from [19] present the average values of the allowable maximum stresses for different mean stresses.

The curves were first normal corrected (by engineering judgment) to represent the lower quartile values. Then the curve presentations were transformed to show the allowable stress amplitude for mean stress. The ratio of the mean stress and the stress amplitude at different numbers of loading cycles N was calculated using the Kossira-Reinke spectrum with 12,5% aerobatics added. Using these values, S-N curves, having a varying stress ratio for the mean stress and the stress amplitude representative for the spectrum, were constructed for the 120 ksi and 180 ksi material data. The S-N curve for the 142,2 ksi material was in-

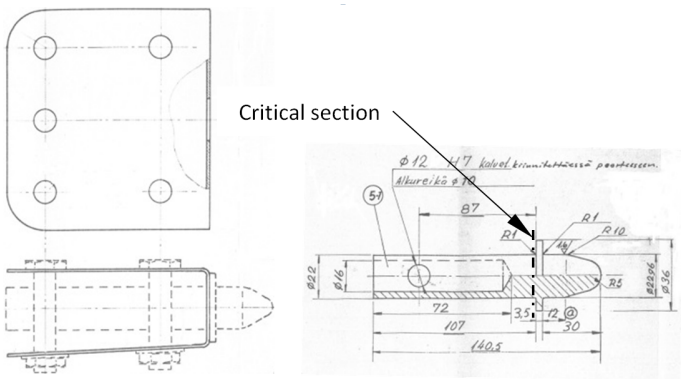

Fig. 12: PIK-20D Wing spar end main fitting bracket.

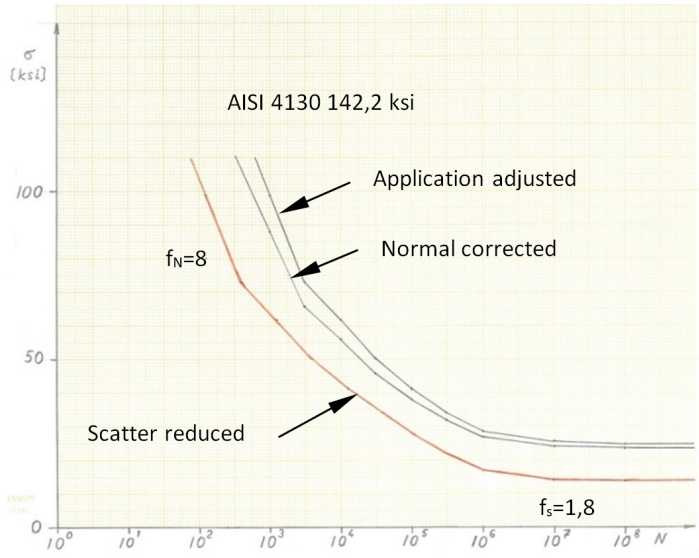

Fig. 13: PIK-20D Wing spar end fitting S-N curves, Soinne [17] (page 36).

terpolated from these two curves and is shown in Fig. 13 as the Normal corrected curve.

In the application adjustment the effects of stress concentration α, volume factor δ, surface roughness factor κ_m and surface treatment factor κ_s were taken into account using expressions (2) to (5).

A reduction of the application adjusted S-N curve was made to take into account scatter. At low cycles, a reduction factor of $f_N = 8$ was used in line with FAAs recommendation. The FAA does not recommend any reduction in stress at high number of cycles. However, to have a comparable reduction at high number of cycles a factor $f_S = 1{,}8$ was applied, which is a severe reduction compared with the common value of 1,3 for metal structures in the Saab method. The Scatter reduced curve is presented in Fig. 13.

The wing spar end fitting fatigue calculation was first based on the 6000 FLH Kossira-Reinke spectrum without aerobatic flight. Using a cumulative fatigue sum limit value $D = 0{,}7$ and a scatter factor of 8 in life and 1,8 in stress the calculation gave a fatigue life of 265655 FLH. When 12,5% aerobatic flight (750 FLH) was added, the fitting fatigue life was reduced to 67607 FLH. Because the critical section is inside of the shoulder fillet and inside of the fitting metal sheet, bolted to the wing spar, it is difficult to inspect. For this reason the wing spar main fitting is a safe life part and must be replaced before reaching the calculated fatigue life.

Tailplane forward fitting bracket

The tailplane forward fitting bracket, shown in Fig. 14, is a welded AISI 4130 alloy steel construction, normalized and annealed to a Tensile Ultimate Strength of $TUS = 67\,\mathrm{kp/mm^2}$ (95,3 ksi). A standard Hirschmann 8 mm rod end in AISI 1213

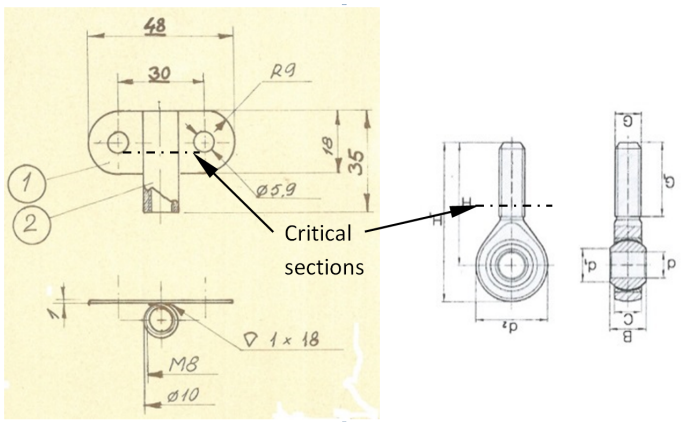

Fig. 14: PIK-20D Tailplane forward fitting bracket and rod end.

steel with $TUS = 520\,\mathrm{N/mm^2}$ (75,4 ksi) is screwed into the fitting bracket.

The rod end and the fitting bracket cylindrical part form a turnbuckle type of joint, where the load transmitted through each thread is not constant along the helix but shows a peak at both ends of the mating threads, see Fig. 15. Compared with a bolt and nut type joint, where there is only one load peak, the total load is divided in two load peaks at half level.

The stress concentration at the thread bottom is due to thread bending and a load bypassing the thread bottom. The geometric stress concentration factor is not easy to estimate as there is a fairly large range in the reported values. The highest value, found in the literature, of $\alpha = 6{,}7$ was utilized, following the recommendation Peterson [20] page 254 of using it with a correction factor for notch sensitivity in a design where fatigue is involved.

The S-N curves were derived by proportioning with Tensile ultimate Strength. The scatter reduced curves contained the factor in life $f_N = 8$ and the factor in stress $f_S = 1{,}8$.

In the application adjustment for the fatigue at the thread bottom the effects of the notch fatigue factor K_f, volume factor δ, surface roughness factor κ_m and surface treatment factor κ_s were

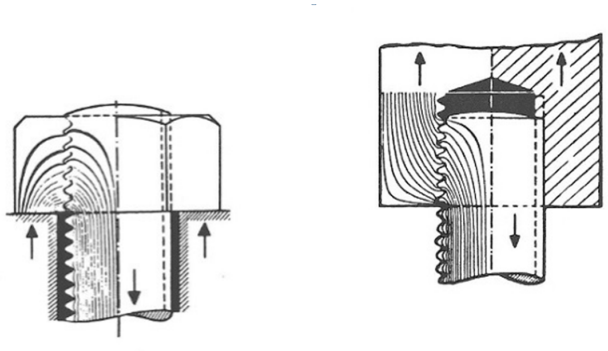

Fig. 15: Stress concentrations in bolt and nut and bolt and turnbuckle type joints.

taken into account. For scratches, tiny holes and radii approaching zero the fatigue strength reduction does not follow the geometric stress concentration factor α, but is taken into account with the fatigue notch factor K_f. Both the fitting bracket and the rod end were checked, the latter being slightly more critical. The thread bottom radius on the rod end is 0,156 mm (0,006 in). In steels the fatigue strength reduction is often relatively small for small notch radii and resulted in a value $K_f = 3{,}239$.

The tailplane forward fitting fatigue calculations were based on the 6000 FLH Kossira-Reinke spectrum with 12,5% aerobatic flight added. The acting stresses in the critical sections through the thread bottom were so low that there was no cumulative damage even at the highest load cycle, because the maximum stress amplitude was lower than the material fatigue endurance limit in spite of the applied scatter factor in stress $f_S = 1{,}8$.

Inspection program

The consequences of the failure of a part were assessed when selecting the inspection objects. The failure of a primary part would cause a loss of the aircraft and at low altitude also the loss of the pilot's life.

On the composite structure primary parts are, for example, the wing spar root, aft fuselage and elevator. On the fuselage quite large damage can be tolerated without losing the aircraft, but not on the wing spar root or the elevator. Also the metal brackets and the control systems were assessed. The wing spar end main fitting bracket pin, wing bevel pins for the attachment of the fuselage and the tailplane forward and aft fitting brackets are primary parts as well as some of the control system parts.

However, the elevator actuator bracket is not a primary part as the elevator push rod acts on the elevator from underneath and the pilot can deflect the elevator upwards and perform a landing. This has been demonstrated several times when pilots have forgotten to connect the elevator push rod in rigging.

The performed analysis of maximum stress areas, strain gage surveys, static test results, fatigue test results, stresses in adjacent elements, stress concentrations and service experience cover the seven point list on page 13 of [16] for the selection of critical inspection areas.

The inspection program was divided into mandatory and voluntary objects to put the emphasis on critical issues. The voluntary objects serve as a guide for good care of the glider on the following facts:

- The combination of fatigue test and analysis, based on measured strains, with a scatter factor in life of $f_N = 8$ and a factor 10 conservative fatigue sum $D = 0{,}1$, yields a fatigue life on the composite structure of at least 938000 FLH based on the Kossira-Reinke spectrum with 12,5% aerobatic flight added.

- The fabrication of wing spar caps in a special tool under pressure, giving a 60% fiber volume and a void free even quality.

- The utilized resin and post curing performed at 70° C, giving a stable structure

- The utilized two-component epoxy paint, giving an improved protection against humidity and UV-radiation compared with gelcoat.

- Fatigue calculations on metal parts with a scatter factor in life of $f_N = 8$ and in stress of $f_S = 1{,}8$ and a fatigue sum $D = 0{,}7$ gave a fatigue life of more than 67000 FLH on the wing spar main fitting based on the Kossira-Reinke spectrum with 12,5% aerobatic flight added. Without aerobatics the corresponding fatigue life exceeds 265000 FLH. Calculations on other brackets did not indicate any cumulative fatigue at all.

- The fatigue test showed that on metal parts there will be on long term backlash due to wear before any indication on fatigue issues thus implying change of parts before fatigue problems.

- Usage of 4130 alloy steel metal parts with stress relieve tempering on welded parts for the avoidance of residual stresses and a passivation and cadmium plating surface treatment yields improved surface protection against corrosion.

- The push rods in aluminum have been given an anodic treatment, the push rods in St 35 steel have been cadmium plated and the sliding push rods in St 35 steel have been chrome plated with sliding drymet bushes in between for improved surface protection.

- The flight flutter tests were performed with 5 mm instead of 6 mm flaperon control line bolts showing that backlash is not an issue for wing flutter.

- Some aircraft have already passed 5000 FLH. The results of special inspections in Finland have not indicated problems.

It was proposed [17] that for a normal condition aircraft the fatigue inspections are started at 10000 FLH with an interval of 5000 FLH until 65000 FLH is reached. At 65000 FLH a renewed review, using future state of the art methods, shall be made by the competent authority to check if this original program is sufficient or if something else is required for the continuation of the inspections and operation of the aircraft or if the inspections can be relaxed. With an annual flight time of approximately 100 FLH reaching the 65000 FLH may take about 500 years. An electronic magnifying glass, indicating the structural fatigue life with six digits, would be great.

Conclusions

PIK-20D glider fatigue tests and calculations have been reviewed thoroughly. The review shows a long fatigue life and that there are no known fatigue problems. To reach a long usage time the metal parts shall be kept free of corrosion, the paint in

good condition to protect the structure against UV-radiation and humidity and the glider shall be stored in dry conditions. A fatigue inspection program [17] has been established to assist in the maintenance.

References

[1] Thielemann, W. and Franzmeyer, F., "Statische und dynamische Festigkeitsuntersuchungen an einem Tragflgel des Segeflugzeuges Cirrus." Bericht 69-02, Institut für Flugzeugbau und Leichtbau, TU Braunschweig, 1969.

[2] Kossira, H. and Reinke, W., "Festigkeit von modernen GFK-Konstruktionen für Segelflugzeuge - Bestimmung eines Belastungskollektivs." Bericht IFL-IB-01, Institut für Flugzeugbau und Leichtbau, Technische Universität Braunschweig, 1984.

[3] Patching, C. and Wood, L., "Fatigue Test of a GFRP Glider Wing." XXII OSTIV Congress, 1991.

[4] Kensche, C., "Fatigue of Composite Materials in Sailplanes and Rotor Blades." *XIX OSTIV Congress, Rieti*, 1985, pp. 57 – 62.

[5] Kensche, C., "Lifetime of GFRP in a shear web and in the girder of a sailplane wing spar." *Technical Soaring*, Vol. 26, No. 2, 2002, pp. 51 – 55.

[6] Kensche, C., "Method of lifetime prediction for sailplane fibre structures." *Technical Soaring*, Vol. 26, No. 2, 2002, pp. 44 – 50.

[7] Kensche, C., "Proposal for a certification procedure of extended sailplane lifetime." *Technical Soaring*, Vol. 26, No. 4, 2002, pp. 94 – 105.

[8] Waibel, G., "Safe life substantiation for a FRP-sailplane." *Technical Soaring*, Vol. 26, No. 2, 2002, pp. 56 – 61.

[9] Nyström, S. and Mai, H., "A fatigue test on a sailplane wing." *Technical Soaring*, Vol. 5, No. 3, 1979, pp. 37 – 42.

[10] Organisation Scientifique et Technique du Vol a Voile, *OSTIV Airworthiness Requirements for Sailplanes*, September 1971.

[11] Holm, I., *Aeronautical course II, strength of materials*, Saab AB, 1979, Lecture notes.

[12] Jarfall, L., *Dimensioning against fatigue, Part I: Normal method*, Swedish Union for Mechanical Engineers, 1977, ISBN 91-524-0368-8.

[13] Lukkarinen, T., *Loading and fatigue analysis of PIK-20 sailplane*, M.Sc. thesis, Helsinki University of Technology, 2008.

[14] Korhonen, H., "Composites as aircraft material and its repair methods." Raisio, 2007.

[15] Lumppio, K., *Life time and usability of a composite aircraft*, M.Sc. thesis, Helsinki University of Technology, 1997.

[16] AFS-120-73-2, "Fatigue evaluation of wing and associated structure on small airplanes." Tech. Rep., Engineering and Manufacturing Division, FAA, May 1973.

[17] Soinne, E., "PIK-20D Fatigue Evaluation." Trafi Research Reports 7/2015, Finnish Transport Safety Agency, 2015, `https://arkisto.trafi.fi/tutkimukset/2015_tutkimukset/pik-20d_fatigue_evaluation` online; accessed 26-October-2018.

[18] Tomblin, J. and Seneviratne, W., "Determining the fatigue life of composite aircraft structures using life and load-enhancement factors." Tech. Rep. DOT/FAA/AR-10/6, U.S. Department of Transportation, Federal Aviation Administration, 2011.

[19] US Department of Defense, *Metallic Materials and Elements for Aerospace Vehicle Structures.*, MIL-HDBK-5j, January 2003.

[20] Peterson, R., *Stress concentration factors*, John Wiley & Sons, 1974.